Supplementary information for: Ultra-fast chemistry under non-equilibrium conditions and the shock to deflagration transition at the nanoscale

Mitchell A. Wood[1,2], *Mathew J. Cherukara*[1,2], *Edward M. Kober*[2], *Alejandro Strachan*[1]

[1]School of Materials Engineering and Birck Nanotechnology Center, Purdue University, West Lafayette, IN 47907, USA

[2]Theoretical Division, Los Alamos National Laboratory, Los Alamos, NM 87545, USA

[‡]Equal Contribution

Corresponding Authors:

Edward Kober (emk@lanl.gov) and Alejandro Strachan (strachan@purdue.edu)

1 Local temperature analysis

The partitioning of the kinetic energies of the atoms into the various components described in the paper was performed as follows:

First the centre of mass velocity of each bin, as described in the Methods Section, is calculated using all the atoms in the bin irrespective of which molecules they belong to.

$$v_I^{cm} = M_I^{-1} \sum_{i \in I} m_i v_i$$

where I is the set of atoms in each bin and $M_I = \sum_{i \in I} m_i$ is the mass of the bin.

Local temperatures are then calculated from the atomic velocities after correcting for their centre of mass motion with respect to the grid.

$$T_I = \frac{2}{3 N_I k_B} \sum_{i \in I} \frac{1}{2} m_i |v_i - v_I^{cm}|^2$$

where k_B is Boltzmann's constant and NI is the number of atoms in bin I.

Once the molecule species are identified through the analysis described elsewhere, temperatures corresponding to each molecule's internal and external degrees of freedom are extracted as follows:

Using the grid corrected velocities of each atom ($v_i^0 = v_i - v_I^{cm}$), the center of mass velocities of each molecule are calculated as follows:

$$v_J^{cm} = M_J^{-1} \sum_{j \in J} m_j v_j^0$$

where J is the set of atoms in each molecule and $M_J = \sum_{j \in J} m_j$ is the molecular mass.

The molecular centre of mass (translational) temperatures for each molecule are then calculated using:

$$T_{CoM} = \frac{1}{3k_B} M_J \left| v_J^{cm} \right|^2$$

It follows then, the intra-molecular (vibrational-rotational) temperatures for each molecule are:

$$T_{vib} = \frac{2}{3(N_{mol} - 1)k_B} \sum_{j \in J} \frac{1}{2} m_j \left| v_j^0 - v_J^{cm} \right|^2$$

where Nmol is the number of atoms in the molecule.

2 Molecular recognition

In order to efficiently describe the large number of chemical processes occurring in these simulations, a distance-based approach was used to identify molecular species. Individual molecules are recognized based on tabulated distance cut offs between atom types. The per-element pairs of distances are taken from the equilibrium structure of the RDX crystal. Care was taken when assigning cut offs to non-bonded pairs in the RDX molecule so that the resultant species were recognized correctly while avoiding over coordinating the parent molecules. Table S1 shows the distance cut offs used to define bonds. When the sample is spatially decomposed as described in the Methods section, a shortened neighbor list can be used to assess the molecular connectivity.

	H	N_{amine}	N_{ring}	O	C
H	1.51	1.65	1.65	1.65	1.25
N_{amine}	-	1.7	1.7	1.4	1.74
N_{ring}	-	-	1.7	1.37	1.74
O	-	-	-	1.6	1.65
C	-	-	-	-	1.75

Supplemental Table S1. Distance based cut offs for RDX used in throughout this study, all values are in units of Angstroms. Two types of nitrogen correspond to their unique locations on the RDX molecule and are treated the same in the ReaxFF parameterization.

To verify our approach we compare its accuracy against a calculation based on the pair-wise bond orders computed by ReaxFF, which acknowledges the information about chemical bonding contained in the simulation. While the bond order approach is more accurate it is also more memory intensive and prohibitive for the void collapse simulations. Figure S2 shows a comparison of molecular species as calculated from the ReaxFF bond orders and those as calculated using the distance cut-off based technique as described in the methods section. Each of these methods to determine bonds in the system are fed through a cluster expansion code that was developed by the authors. We compare the calculated decomposition profiles for 3 cases of amorphous RDX ignited at 1500 K at densities of 1.62 g/cm^3, 1.96 g/cm^3 and 2.12 g/cm^3. As seen in the figure, populations calculated from the atomic distances are in excellent agreement to molecular species identified from the bond orders. One thing worth noting is that small molecules are more cleanly identified at high pressures due to the low occupancy volume of say N_2 or CO_2 moieties. A further advantage of our technique is the ability to post-process these analyses, allowing the analysis of each frame concurrently. These cook-off simulations agree well with previous RDX decomposition work from reactive MD from Strachan *et. al.*[4], though their work was concerned with crystalline RDX which is in contrast to these amorphous cases shown in Figure S2. Still, our observed time decay of the potential energy curves are in good agreement with their results wherein an exponential decay constant of 248-276ps was calculated

for crystalline densities between 2.11 and 1.68 g/cm^3. These amorphous cook off simulations also capture the same general trend of decreasing reaction timescales for increasing density which was also seen from Strachan *et. al*.[4].

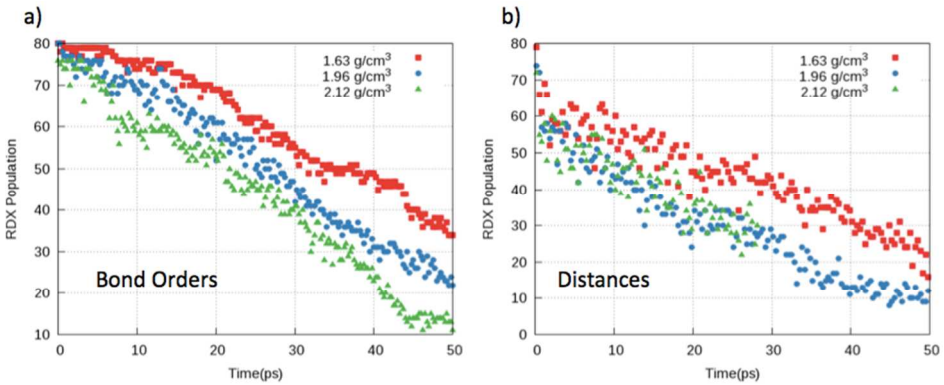

Supplemental Figure S2. Populations of RDX over time at different densities calculated using the ReaxFF bond orders a) and b) RDX populations calculated using atomic distances.

2. Validation of the ReaxFF description of energetic materials

Although a well-tested technique, molecular dynamics simulations have inherent limitations; the foremost are the length (sub-micrometer) and time (sub-micro second) restrictions. In addition, reactive potentials have to be trained to represent a large number of configurational and reactive states wherein experimental and ab initio data have to be extrapolated. A primary cause of concern is reactions at extreme conditions where the potential energy surface description may not be well characterized, nor could it be from the training set. By contrast, the extensive training set of first principles data that goes into the force field used here captures the vast majority of reaction paths, including NO_2 loss, HONO elimination and ring opening paths that are known at temperatures and pressures relevant to shock compression. Quantitative comparisons of these reaction paths can be found here [3,4].

To test the accuracy of the ReaxFF potential used in the simulations in the description of the decomposition of energetic materials under pressure and temperature such as those seen in the vicinity of the collapsed pore, we compare rates of decomposition and of product formation to electronic-structure-based simulations for HMX[1] and nitromethane[2]. We note that, as discussed in Section 1.3, this ReaxFF parameterization that adds multi-molecular reactions to the training set lead to similar results to a previous parameter set use in Ref. [4].

2.1 Comparison of predicted reaction rates of HMX

The initial conditions simulated corresponded exactly with the simulation setup described in the paper, with the only exception being the number of molecules used in the simulation (48 instead of 6). The initial conditions correspond to a temperature of 3500 K and a density of 1.9 g/cm^3. SM Figure 5 shows the results of our simulations (normalized to account for the difference in simulation size) and those contained in the reference paper.

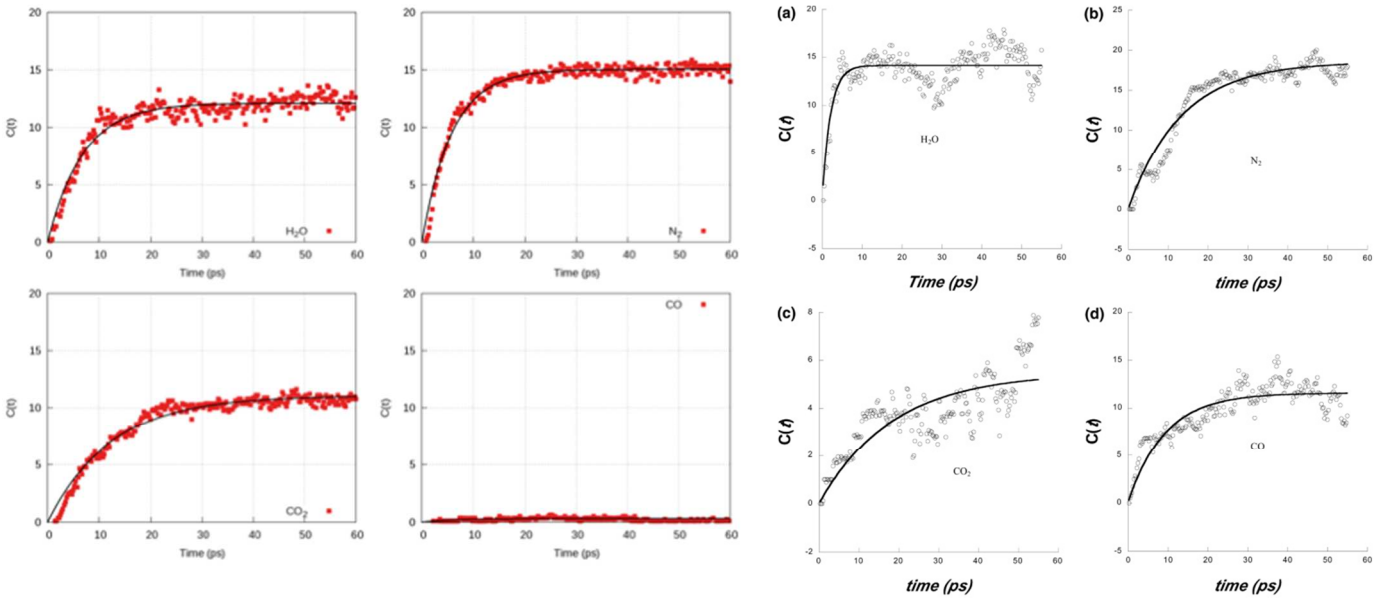

Supplemental Figure S8. Populations of product species a) H_2O, b) N_2, c) CO_2 and d) CO as predicted by first principles calculations and e),f),g),h) as predicted by this potential. Plots a), b)

c) and d) are reprinted with permission from Manaa, M. R., Fried, L. E., Melius, C. F., Elstner, M. & Frauenheim, T. Decomposition of HMX at Extreme Conditions: A Molecular Dynamics Simulation. J. Phys. Chem. A **106,** 9024–9029. Copyright 2002 American Chemical Society.

We find semi-quantitative agreement with the DFTB results except for the populations of CO and CO_2, where we predict the formation of larger amounts of CO_2 than CO. However, this preference for CO_2 production is predicted by thermodynamical calculations such as those implemented in the Cheetah code. SM Figure 6 shows a comparison of the populations of different species across the three types of theory. As can be seen, the predictions of this force field are comparable in most respects to the experimentally calibrated models.

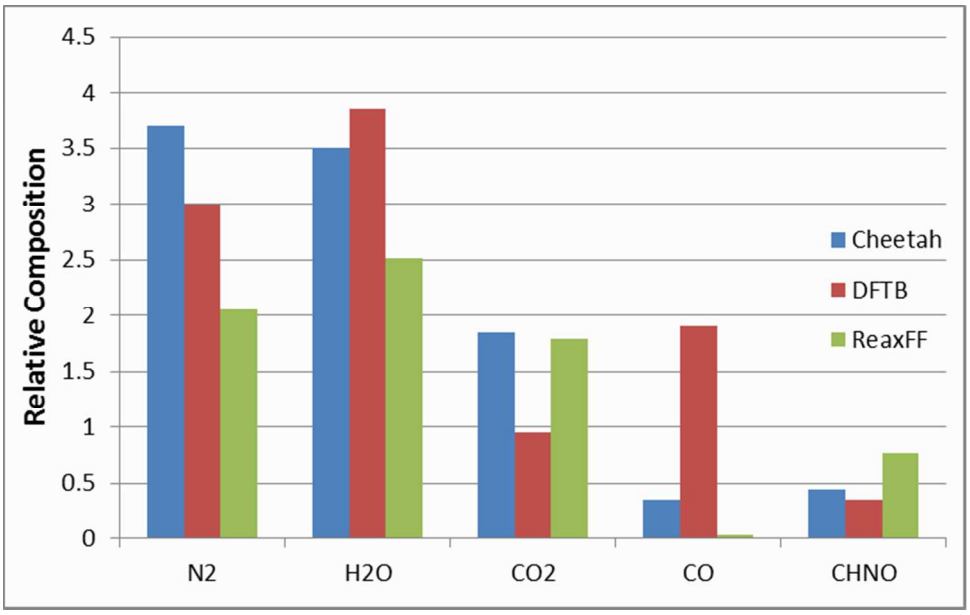

Supplemental Figure S9. Comparison between thermodynamic calculations, DFTB and ReaxFF data. Data corresponding to DFTB and Cheetah have been taken from Manaa, M. R., Fried, L. E., Melius, C. F., Elstner, M. & Frauenheim, T. Decomposition of HMX at Extreme Conditions: A Molecular Dynamics Simulation. J. Phys. Chem. A **106,** 9024–9029. Copyright 2002 American Chemical Society.

2.2 Comparison of predicted reaction rates in nitromethane

For our second test of the veracity of the potential in capturing reaction kinetics of HE materials at extreme conditions of temperature and pressure, we recreate the simulation setup described in this reference[2]. As before, the simulation cell chosen is 8 times the cell in the reference, and we normalize the populations to compare with the original data. Here, we compare the reaction rates for a sample of NM heated to 4000 K and compressed to a density of 2.2 g/cm^3.

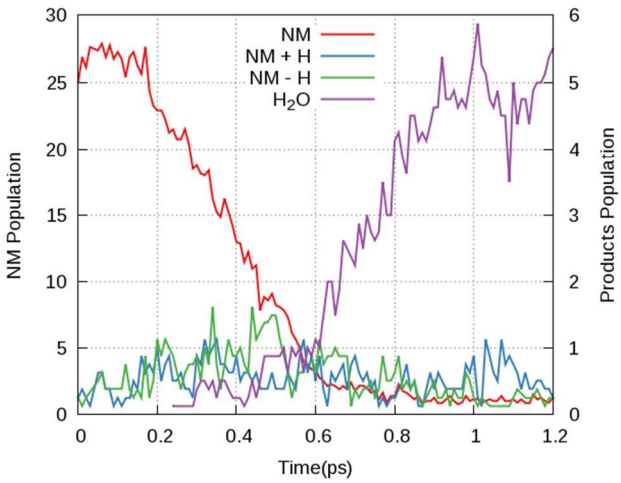

Supplemental Figure S10. Species populations as a function of time in thermally initiated NM as predicted by this potential.

As a comparison to Figure 5 in Reference 2 shows, this potential captures well the overall kinetics of the decomposition of the nitromethane, the relative populations of the protonated and de-protonated molecules, as well as the rate of formation of the product species.

3. Supplementary movies:

Supplementary movies complementing Figures 1 and 2 are provided, showing the local evolution in the system with a resolution of 0.1 ps.

SM 1: Local averages of T_{com}

SM 2: Local averages of T_{vib}

SM 3: Local fractions of RDX molecules

SM4: Local fractions of the intermediate species (NO_2, NO, OH, HONO, COOH)

SM 5: Local fractions of product species (N_2, O_2, CO_2 and H_2O)

SM 6: Close up view of the molecular species formed in the vicinity of the pore. RDX molecules are not shown for clarity. NO_2 is in red, OH is in pink, H_2O is in light blue, N_2 is in green and CO_2 is in dark blue.

SM 7: Temperature evolution of the artificial crescent shaped hot spot used in Figure S4 a-c

SM 8: Temperature evolution of the dynamically formed hot spot shown in Figure S4 d-f

SM 9: Temperature evolution of the 5nm cylindrical artificial hot spot shown in Figure S5

SM 10: Temperature evolution of the largest cylindrical artificial hot spot shown in Figure S6

REFERENCES

1. Manaa, M. R., Fried, L. E., Melius, C. F., Elstner, M. & Frauenheim, T. Decomposition of HMX at Extreme Conditions: A Molecular Dynamics Simulation. *J. Phys. Chem. A* **106,** 9024–9029 (2002).

2. Manaa, M. R., Reed, E. J., Fried, L. E., Galli, G. & Gygi, F. Early chemistry in hot and dense nitromethane: molecular dynamics simulations. *J. Chem. Phys.* **120,** 10146–53 (2004).

3. Wood, M., van Duin, A. C. T. & Strachan, A. Coupled Thermal and Electromagnetic Induced Decomposition in the Molecular Explosive αHMX; A Reactive Molecular Dynamics Study. J. Phys. Chem. A 118, 885 (2014).

4. Strachan, A., Kober, E. M., van Duin, A. C. T., Oxgaard, J. & Goddard, W. A. Thermal decomposition of RDX from reactive molecular dynamics. J. Chem. Phys. 122, 54502 (2005).